Enhancing the Cavitation Erosion Resistance of 304 Stainless Steel by Laser Surface Alloying with Molybdenum

Bori, I.[1]; Muriana, R.A.[2], Man, H.C.[3]; Okegbile, O.J.[1]; Ayo, S.A.[1]; and Alkali, B.[1]

[1] Department of Mechanical Engineering, Federal University of Technology, Minna, Nigeria

[2]Department of Materials and Metallurgical Engineering, Federal University of Technology, Minna, Nigeria

[3]Department of Industrial Systems Engineering, the Hong Kong Polytechnic University, Hong Kong

E-mail: ige.bori@futminna.edu.ng

Abstract

Type 304 stainless steel is the most versatile and widely used austenitic stainless steel, it accounts for more than 50% of all stainless steel produced. It is commonly used in liquid-handling equipment, house hold utensils and lot of applications in almost every industry. However, poor surface properties in terms of wear resistance, due to its low hardness made it susceptible to cavitation erosion, which is a usual mode of degradation of engineering parts in contact with fast-flowing or vibrating liquids. This work is an attempt to improve the cavitation erosion resistance of 304 stainless steel by laser surface alloying with Molybdenum (Mo). This was made possible by using a 2kW continuous wave Nd-YAG laser. The alloying powder was placed in advance on the surface of the substrate by pasting to a thickness of 0.1mm, followed by laser beam scanning at an optimal speed of 20 mm/s and 30 mm/s (each at a beam diameter of 3mm) and a laser power of 1.2kW, in order to achieve surface alloying and modified surfaces were obtained by 50% overlapping of adjacent tracks. The microstructure and composition of modified layer were also studied for more insights. Ultrasonic induced vibrator tester was used to carry out cavitation erosion test. Cavitation erosion resistance (Re) was observed to have increased with the Mo content in the alloyed layer, the Re of the specimens modified with Mo was improved by a factor of 1.4 (for v = 20 mm/s) and 1.5 (for v = 30 mm/s), when compared with that of the as-received 304 stainless steel substrates.

Keywords: Cavitation, Laser, Alloying, Molybdenum, Stainless Steel.

Introduction

Type 304 stainless steel is the most widely used among the austenitic stainless steels, for both domestic and industrial usages, where they are bound to have contact with high flowing fluids and corrosive liquids especially those containing chlorides, thereby causing quick material failure as a result of cavitation erosion and corrosion occurring at its surfaces. Attack due to cavitation erosion is a common problem in engineering parts in contact with a liquid, and its mechanism is summarized in six steps shown in Fig.1.

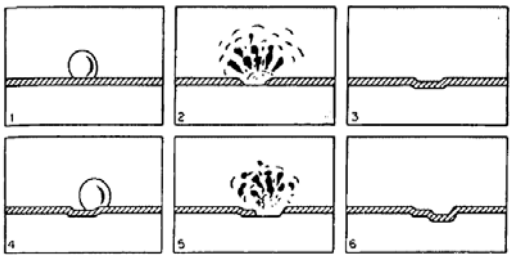

Fig. 1: Schematic representations of steps in cavitation erosion (Fontana, (1987)).

(i) A cavity forms on the protective film of a metal, (ii) The cavity collapses and destroys the film, (iii) The newly exposed metal surface corroded and the film is reformed, (iv) A new cavity forms on the same site, (v) The cavity collapses and

destroys the film, and (vi) The exposed area is corroded and the film is reformed. The repetition of cavitation erosion results in deep crater.In general, the damage due to cavitation erosion may be mitigated via improvement of the hydrodynamic design and/or the use of more resistant materials. While both approaches are feasible, they have inherent limitations, especially when cost and other factors come into consideration. As cavitation erosion occurs at the solid/liquid interface, only the properties of the surface layer, but not the bulk, contribute to the cavitation erosion resistance of a solid.

In view of this, it is obvious that surface modification techniques naturally offer another route to combat cavitation erosion. Surface modification techniques are especially attractive in engineering applications as they only consume a small amount of precious materials on the surface while retaining the bulk properties of the treated parts, thus reducing the cost and at the same time providing a large number of combinations of surface and bulk properties which may be tailored for specific purposes. Other advantages include minimum heat input, a clean process and an efficient but not labor intensive process. In the time past, the following techniques had been employed by various groups to modify the surface layer for increasing cavitation erosion resistance namely: electroplating (Okada *et al.,* 1988), ion implantation (Gately & Dilich, 1987), ion-plating (Matsumura *et al.,* 1990), explosive welding (Richman & McNaughton, 1997), thermal spraying (Guo *et al.,* 1989, Sang & Li, 1995).Owing to a number of special features, laser treatment has emerged as a popular technique in surface modification.

Laser surface modification derives its attractiveness in engineering applications mainly from: (i) the formation of a small heat-affected zone, thus leaving the bulk properties unchanged and introducing minimal distortion; (ii) refinement and homogenization of microstructure, leading to enhanced mechanical properties; and (iii) the possibility of forming novel surface alloys unattainable by other methods because of the non-equilibrium nature of the process. Relatively high rate of processing, ease of automation, possible operation at atmospheric pressure and the localized nature of laser treatment are additional advantages over conventional surface modification techniques.

In view of these advantages, laser surface modification has been employed by several authors in improving the cavitation erosion resistance of some structural materials. Examples of such an attempt include the laser surface melting (LSM) of iron and steel (Gadag & Srinivasan, 1995; Giren, 1998), aluminum alloy (Tomlinson & Bransden, 1995), and titanium alloy (Robinson *et al.,* 1995), with the degree of improvement in cavitation erosion resistance comparable to those using conventional techniques. In addition, some past works involving laser surface alloying of 304 stainless steel include: (i) laser composite surfacing with titanium boride (Majumdar *et al.,* 2007), (ii) tribocorrosion behavior of duplex surface treated (Frutos *et al.* (2010), (iii) Hard TiC coating (Ushashri & Manoj, 2015), (iv) FeCoCrAlNiTix high entropy alloy coatings (Wu *et al.,* 2017), (v) Cr-Ni-Mo-Cu cladding (Xu *et al.,* 2012) and (vi) FeCoCrAlNi high-entropy alloy coatings (Zhang *et al.,* 2016). The motivation for this work is that, literature (Zhang *et al.,* 2014) had already established the fact that, 304 stainless steel has poor surface properties in terms of wear resistance, due to its low hardness made it liable to cavitation erosion. Admittedly, 304 stainless steel does not contain any of the hard metallic elements such as Molybdenum (Mo) or others in its chemical composition, which could have contributed to its cavitation erosion resistance enhancement, as a result of improved surface hardness.

In view of this, Molybdenum (Mo) was chosen as the surface alloying element in this study, because of its unique hardness

property, and its ability to resist corrosion at ordinary temperatures. The essence of doing this is to enhance the cavitation erosion resistance of 304 stainless steel, via surface hardness improvement first. This approach is supported from the previous work (Richman & McNaughton, 1990) on correlation between hardness and cavitation erosion resistance results, obtained.

.

Materials and Method

Substrate Material and Specimens Preparation

The substrate material used in this study was a 304 stainless steel. Also for the purpose of comparison only, 316 stainless steel containing 3% Molybdenum was also considered. Chemical (elemental) compositions of as-received 304 stainless steel as determined by Energy-Dispersive Spectrometry (EDS) are shown in Table 1: While the chemical compositions of as-received 316 stainless steel are shown in Table 2:

Table 1: Percent Chemical (elemental) Compositions of As-Received 304 Stainless Steel

Fe	Cr	Ni	Mn	Mo	Si	C	P	S
70.85	18.0	8.0	2.0	-	1.0	0.08	0.045	0.03

Table 2: % Chemical (elemental) Compositions of 316 Stainless Steel

Fe	Cr	Ni	Mn	Mo	Si	C	P	S
61.85	18.0	14.0	2.0	3.0	1.0	0.08	0.045	0.03

As-received 304 stainless steel was cut into rectangular bars with dimensions 50 mm x 50mm x 5mm, with the aid of a power hacksaw. The surface of specimens for laser surface alloying was sand-blasted in order to remove any form of impurities, oxides deposit and to promote preplaced powder adhesion in laser surface alloying. After that, specimen surfaces were thoroughly washed with water and dried.

Molybdenum Powder Replacement

An appropriate amount of Mo powder was mixed with a binder (polyvinyl alcohol, PVA) to form a gel-like slurry. The viscosity of slurry was a decisive factor in the overall quality of powder pre-placement. That is, sticky slurry would prevent the powder to be placed evenly over a large sample area while fluid slurry means insufficient Mo powder for the alloying process. When mixed with the PVA solution, air bubbles would inevitably be trapped inside the slurry and due to the viscous nature they would be very difficult to get rid of. However, during painting, the sample could be tapped slightly in order to (i) get rid of trapped air bubbles and (ii) let the viscous slurry to spread out evenly. In order to achieve a uniform thickness of 0.1mm for the coated slurry, masking tapes each of 0.1mm thickness were glued parallel at the opposite ends of the specimen surfaces, then the slurry was pasted in between the tapes (with same level), and finally dried inside an oven at a temperature of 70^{o}C for 5 hours.

Laser Surface Treatment

An Nd:YAG laser (JK MultiWave^{TM}, Lumonics, MW2000) was employed for laser surface treatment. The laser can

achieve a maximum mean output power of 2 kW in the continuous wave (CW) mode. However in the current study, a laser power of 1.2 kW on work piece was selected as an optimized operating condition. The laser system comprises of a single enclosure housing of top-mount laser head, with power and control electronic modules and the cooling system underneath. Laser output is delivered by a single fibre optic cable which exits through an output connector on the laser head lid.

The effect of back reflection is significant when processing material with high reflectivity such as aluminum and copper-alloys. The consequences include overheating and permanent damage to fibre head. Back reflection from the work piece is prevented by carefully adjusting the optical axis to tilt 10^{o} relative to the normal direction of work piece. Inert gas (Argon (Ar)) shielding was provided simultaneously during alloying. It was employed for two purposes: (i) to remove residue on the work piece and (ii) prevent oxidation of the surface being processed. Fig. 2 illustrates the set-up of the focusing head and its relation to work piece.

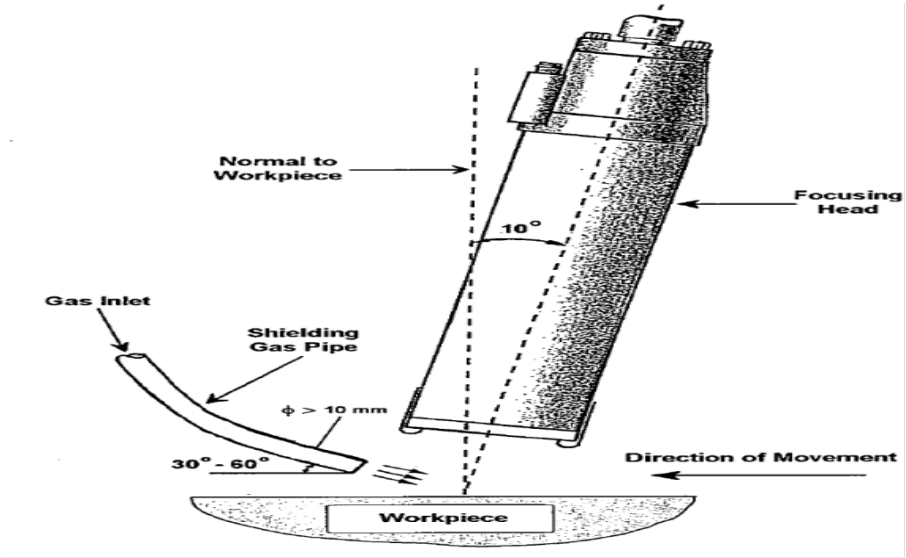

Fig. 2: Schematic drawing showing the configuration of focusing head, position of gas shielding feed in relation to work piece(Tam *et al.*, 2002).

Laser Surface Alloying

Laser surface alloying was performed using a laser power of 1.2 kW with a beam size of 3mm in diameter and beam scanning speeds of 20mm/s and 30mm/s, i.e. optimized processing speeds, after trying a series of single track scanning speeds, while other parameters such as laser power and laser spot diameter remain constant, based on which single track scanning speed would produce a higher surface hardness for the modified surface than the as-received AISI 304 Stainless steel. The laser beam was conveyed by optical fibre and focused onto the specimen by a Zinc Selenide (ZnSe) lens with focal length of 100mm. Argon was employed as a shielding gas at a flow rate of 20 lit/min and pressure of 40 Psi. Laser surfacing was obtained by parallel tracks with 50%

overlap as shown in Fig. 3; such an overlapping ratio was considered so as to optimize surfacing efficiency and surface homogeneity. More on the effect of overlapping factor on melting ratio in laser cladding had also been investigated by Farnia *et al.* (2013).

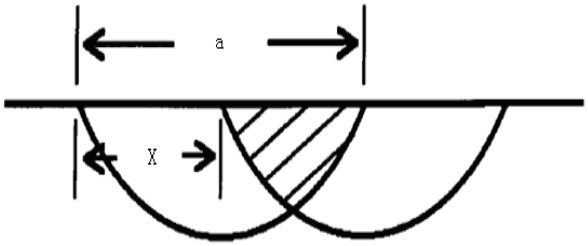

Fig. 3: Overlapping of single tracks.

where the overlapping ratio is defined as:

$$\text{Overlapping ratio} = \frac{(a-x)}{a} \quad (1)$$

a is the width of a single track and x is the displacement between adjacent tracks. When the overlapping is small, homogeneity of the treated surface will be affected. On the other hand, a large overlapping ratio makes the surfacing process inefficient.

Metallographic and Microstructural Analysis
Optical Microscopy (OM)
The laser treated specimens were sectioned, mounted in a hot-curing epoxy holder, grinded (starting with 60 grit to 800 grit SiC papers), polished and etched with a Marble reagent solution (4 g CuSO4, 20 ml HCl and 20 ml H_2O) for 10-30 seconds. Then the specimens were observed by optical microscopy, with a "Leica DMLM" microscope at a magnification of 2.5 times. The microstructures of laser treated specimens were analyzed; the melt depth and width of the specimens were measured with the aid of incorporated software called "Leica Qwin", for image processing and analysis.

Scanning Electron Microscopy (SEM)
SEM, which can give a higher magnification up to 10,000 times (Leica, Stereoscan 440), was used as a supplement to OM for the study of the microstructures of laser treated specimens. The mounted specimens were gold-coated for electrical conduction in the study of SEM. Moreover, surface morphology before and after Cavitation test were studied by SEM.

Energy Dispersive X-Ray Spectroscopy (EDS)
When the high energy electrons produced in SEM interact with the atoms within the top few micrometer (μm) of the specimen surface, X-rays are generated with an energy characteristic of the atom that produces them. The intensity of such X-ray is proportional to the mass fraction of that element in the specimen. Therefore, the chemical compositions of specimens were determined by the energy dispersive X-ray spectroscopy (EDS) together with SEM. The elements with atomic weight higher than sodium (Na) can be studied. The light elements (atomic weight lower than Na) such as B and C can be analyzed with a windowless detector. The average chemical compositions of laser treated specimens were taken at five to six points (depending on the melt depth) from top to bottom of melt zone, at an interval of 120 μm between point

Vickers Microhardness Testing
To determine the hardness of a phase or the hardness profile along the depth of the

cross-section, the Vickers hardness HV number is calculated according to the equation in ASTM Standard E, (1999) as follows:

$$HV = 1854.4X\,P/d^2 \qquad (2)$$

where P **is** the load in gf and d is the mean diagonal distance of the indentation in µm (Fig. 4 (a)). The indentation test would also provide qualitative information on the fracture toughness of the modified layer by observing if cracks are present (Fig. 4 (b)), and also the degree of cracking.

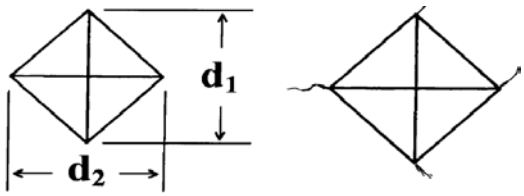

(a) (b)

Fig. 4: Vickers indentations (a) the indent, (b) cracks due to indentation.

In this study, a load of 300g was applied at a loading time of 15 seconds for each point within the melt zone, at an interval of 100 µm between points.

Cavitation Erosion Testing
Ultrasonic Induced Vibrator Tester

An ultrasonic induced vibrator cavitation facility (Heat System Inc. U.S.A. Sonicator Ultrasonic Liquid Processor Model XL2020, 550 W) was employed to carry out the cavitation erosion experiments. As shown in Fig. 5, the cavitation erosion tester consists of a power supply, a converter and a disrupter horn. The power supply converts conventional 50 or 60 Hz alternating current to 20 kHz electrical energy fed to the converter, which transforms the electrical energy to mechanical energy.

The cavitation erosion test was performed conforming to the already established standard (ASTM Standard G 32-92, 1995), with minor adjustment in the method of mounting the specimen. Instead of mounting the specimen directly to the ultrasonic horn, it was held stationary at a distance 1 mm below the horn. Such a method has also been used by some other researchers (Tam *et al.*, 2002). The vibratory studs were made of super duplex stainless steel S32760 and the setup is shown in Fig. 5, the vibratory frequency used was 20 kHz and the peak to peak amplitude was set at 50 µm by a dial indicator. The specimens were made to pass through a series of cavitation erosion tests in 3.5% NaCl (i.e. dissolved 35 g of NaCl in 1000ml of deionized water at 23^{o}C).

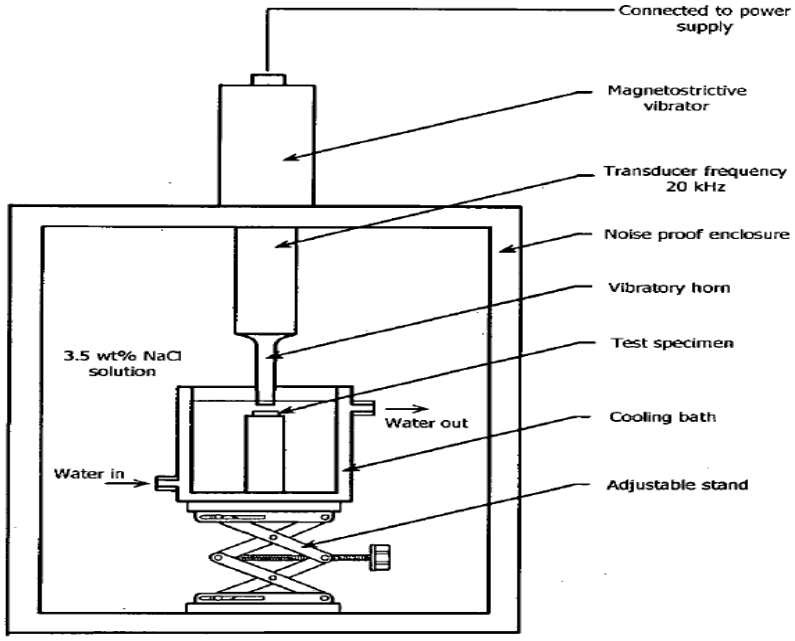

Fig. 5: Schematic diagrams showing the setup of cavitation erosion test.

Evaluation of Cavitation Erosion Resistance

Subsequent to the cavitation test, the specimens (as-received 304 stainless steel, 316 (for comparison) stainless steel and laser treated) were cleaned, degreased, dried and weighed at each interval of the test. Weight loss at each time interval was obtained by weighing the specimens using an electronic balance with accuracy of ±0.1 mg (METTER AT balance). Each cavitation erosion test was completed after 4 hours, which included four intermittent periods each of an hour. The specimens were weighed at regular interval of 1 hour. The erosion loss of materials was expressed in terms of the mean depth of penetration (MDP) and the mean depth of penetration rate (MDPR) as calculated by the following equations:

$$MDP\ (\mu m) = \frac{\Delta W}{10\rho A} \qquad (3)$$

and

$$MDPR(\mu m/h) = \frac{\Delta W}{10\rho A \Delta t} \qquad (4)$$

where ΔW is the weight loss at each time interval in mg, Δt is the time interval in hours, A is the surface area of the specimens in cm^2 and ρ is the density of the modified melt layer in gcm^{-3}.

The cumulative MDP versus time curve could then be calculated. In addition, the cavitation erosion resistance R_e is defined as the reciprocal of the mean depth of penetration rate.

$$R_e(h/\mu m) = (MDPR)^{-1} \qquad (5)$$

Results and Discussion

Metallurgical and Metallographic Analysis

Optical Microscopy

After laser irradiation, the alloy powder (Mo) and the underneath 304 substrates were melted and intermixed, and quickly solidified to form a modified layer. Morphologies study of 304 stainless steel subjected to cavitation erosion test was also carried out by Zhang *et al.* (2017). First observation to be made was that, the melt zones were more resistant to etching reagent, that is, it took more time (between 20-30 seconds) to etch the modified layer, compared with time for etching the as-

received 304 stainless (5-10 seconds). The microstructure of as-received 304 is shown in Fig. 6 (which is meant to show the different phases present, but not meant to represent the proportions of these phases). Sectional views of the melt zones after etching are shown in Fig. 7. With the aid of an optical microscope, numerical values of the width (μm) and depth (μm) of the melt zones were also determined and are given in Table 3, showing that, the higher the laser scanning speed, the lower the depth of the melt zone. Black dots noted within the melt zones is due to the formation of carbide, that is, chemical reaction between iron (Fe) and Carbon (C).

Fig. 6: Optical micrograph showing the microstructure of as-received 304 stainless steel.

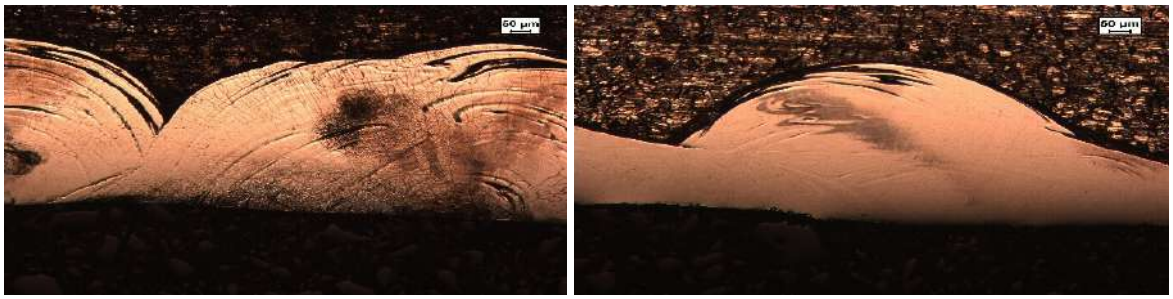

(a) (b)

Fig. 7: Sectional views of the melt zones (a) with laser scanning speed of 20 mm/s; (b) with laser scanning speed of 30 mm/s.

Table 3: Melt Zones' Parameters

Scanning speed (mm/s)	Depth of melt zone (μm)	Width of melt zone (μm)
20	615.36	2210.27
30	285.06	2021.18

SEM after laser surface alloying

The SEM micrographs of Molybdenum-304 (Mo-304) stainless steel cross sectional view after laser surface alloying, at different part of the melt zones are shown in Figs. 8 and 9 respectively. From the top of the surface, the laser surface alloyed specimens consisted of the melted zone (MZ), the partially molten transition zone (TZ), the heat-affected zone (HAZ) and the substrate.

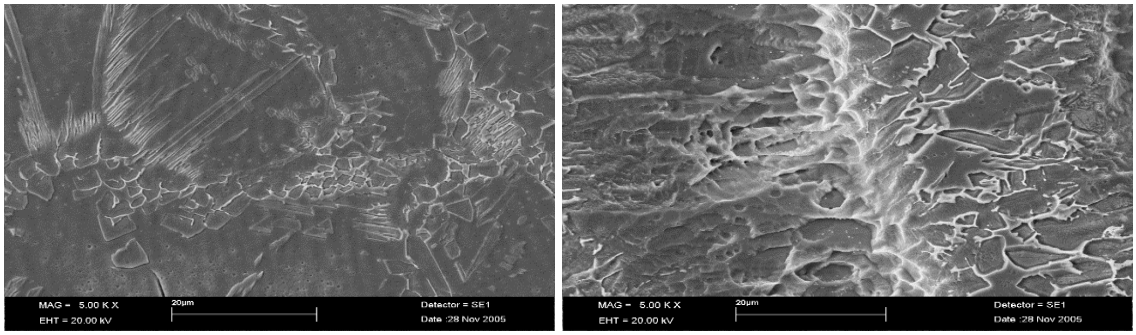

(a) (b)

Fig. 8: SEM micrographs of Mo-304 stainless steel after Laser surface alloying when v = 20 mm/s: (a) middle part of the melt zone; (b) interface between successive melt layers.

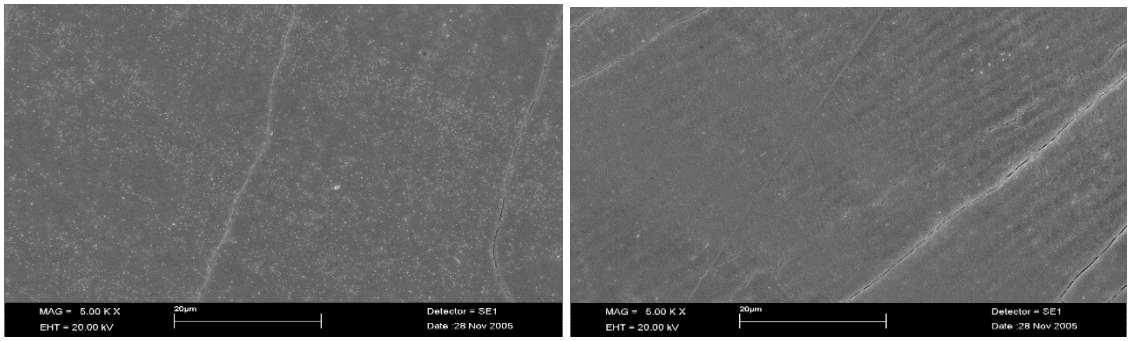

(a) (b)

Fig. 9: SEM micrographs of Mo-304 stainless steel after Laser surface alloying when v = 30 mm/s: (a) middle part of the melt zone; (b) interface between successive layers.

From the SEM micrographs, it is observed that, the degree of melting at v = 30 mm/s between the alloy powder (Mo) and the underneath substrate is quite low, compared to when v = 20 mm/s. This shows that low laser scanning speed is much efficient for laser surface alloying process.

EDS Composition Analysis of Laser Surface Alloyed Mo– 304 Stainless Steel

The EDS profile along the depth of the cross-section is shown in Fig. 10, which shows that the alloyed zone is rich of Molybdenum with an average weight of 8.86% and 11.29%, at a laser scanning speeds of 20 mm/s and 30 mm/s respectively, compared with as- received 304 stainless steel which contain no Molybdenum in composition and even 316 stainless steel that only contains maximum average weight of 3% Mo. In addition, the Mo wt% compositions obtained within the laser alloyed modified surfaces in this work, were more than any stainless steel with Mo wt% composition, according to the literature (Lovland, 1993). The EDS results show that a surface alloy of Mo-304 stainless steel is more pronounced in the case of lower laser scanning speed of 20 mm/s, as penetration of Mo into the substrate is deeper and almost remain within an average weight of 8.86%, which implies a better surface alloying.

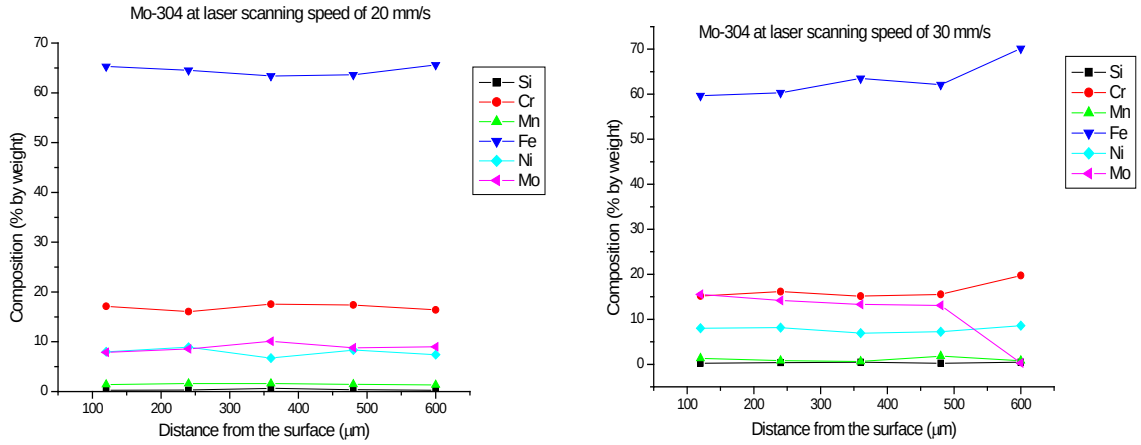

(a) (b)

Fig. 10: EDS Composition profile along the depth of alloyed zone Mo-304 stainless steel (a) At a laser scanning speed of 20 mm/s; (b) at a laser scanning speed of 30 mm/s.

Microhardness (HV) of the Alloyed Layers

The microhardness values of five measurements taken for each specimen, when a load of 300g was applied at a loading time of 15 seconds for each point, along the depth of the cross-section of the modified specimens are shown in Fig.11. Owing to the presence of the carbides, and the refined microstructure due to the high cooling rate typical of laser treatment, the microhardness HV of the alloyed layers are significantly increased, from a value of 295 HV for as-received 304 stainless steel to approximately average of 359 HV and 385 HV for the laser-treated specimens, at laser scanning speeds of 20 mm/s and 30 mm/s respectively.

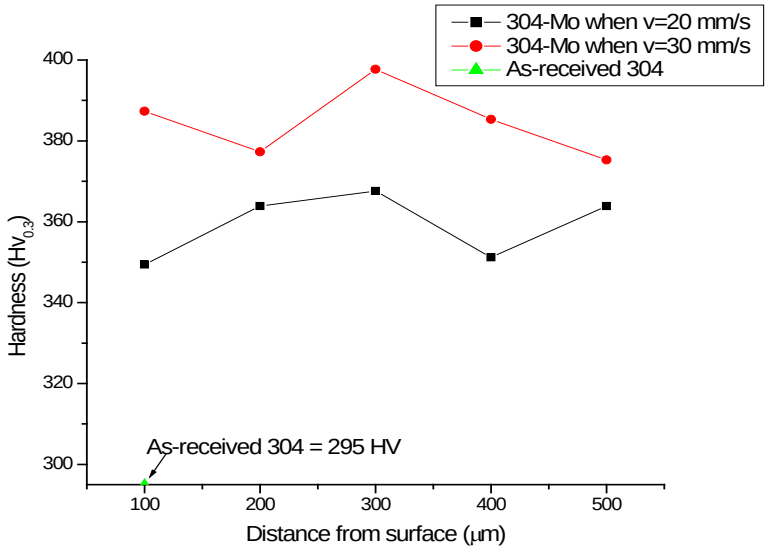

Fig. 11: Hardness profiles along the depth of the cross-section of the modified specimens.

The Vickers indentations from optical micrographs shown in Fig. 12 provide some information on the fracture toughness of the alloyed layers. The alloyed layers in both specimens are not brittle, as there is no evidence of cracks around the indentations. This points out that an appropriate compromise between hardness and fracture toughness or ductility (opposite to brittleness) would lead to high cavitation erosion resistance, as has been pointed out by Wang *et al.* (1991).

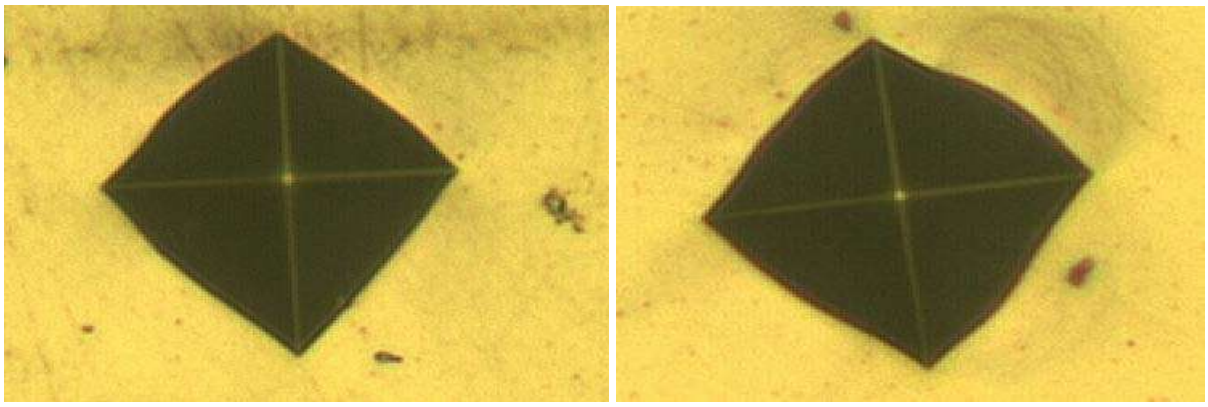

(a) (b)

Fig. 12: Optical micrographs of Vickers indentationsof Mo-304 stainless steel surface alloyed: (a) for v = 20 mm/s; (b) for v = 30 mm/s (both at 300-g load).

Cavitation Erosion Resistance

At the end of the cavitation erosion test, equations (3) to (5) were used to calculate the values of mean depth of penetration (MDP), mean depth of penetration rate (MDPR) and the cavitation erosion resistance (Re) respectively, for each cavitation erosion test completed after 4 hours, which included four intermittent periods each of an hour. As-received 304 and 316 (containing 2-3% Mo) were also tested for comparison purposes. Fig. 13 shows the cumulative MDP of the as-received 304 and 316 stainless steels, and the laser surface modified Mo-304 stainless steel specimens (when v=20 mm/s and 30 mm/s) cavitated in 3.5% NaCl solution at 23^{o}C as a function of time. The obtained cavitation erosion resistance (R_e) values for as-received 304 and 316 stainless steel specimens, and that of laser modified surfaces with Molybdenum (Mo) at different scanning speeds are shown in Table 4.

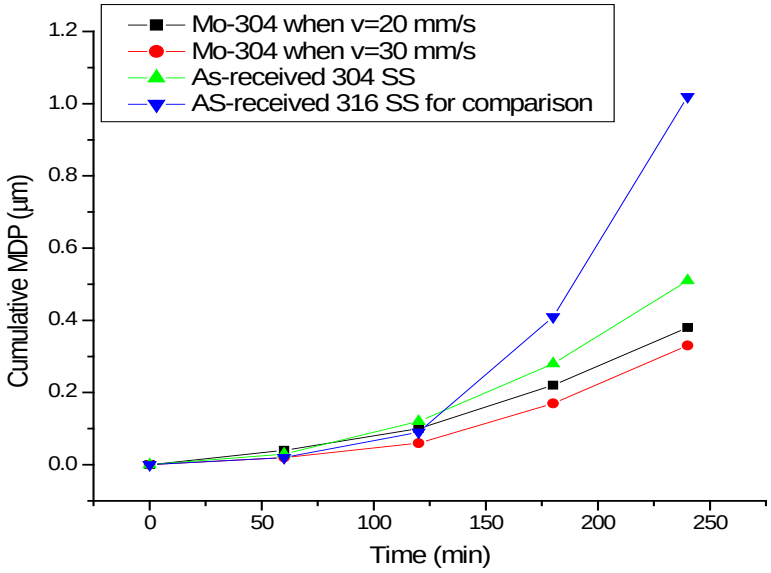

Fig. 13: Cumulative mean depth of penetration (MDP) as a function of time for the as-received and laser surface modified specimens eroded in 3.5% NaCl solution at 23^{o}C.

Table 4: Cavitation Erosion Resistance (R_e) Values

Specimens	$R_e(h\mu m^{-1})$
As-received 304 stainless steel	17.0
As-received 316 stainless steel	7.0
Mo-304 stainless steel laser surface alloyed (for v = 20 mm/s)	24.0
Mo-304 stainless steel laser surface alloyed(for v = 30 mm/s)	26.0

By normalizing the R_e values with respect to that of as-received 304 stainless value, the cavitation erosion resistances improved about 1.5 and 1.4 times that of the as-received 304 stainless steel, for the laser modified surfaces with Mo, for when the scanning speeds are $30\,mm/s$ and $20\,mm/s$ respectively. The improvement in cavitation erosion resistance was consistent with the increase in hardness of the laser modified surfaces. Surface morphology of the eroded surfaces after 4 hours of cavitation test is shown in Fig. 14. Similar SEM approach was also applied in the previous investigation of Abouel-Kasem *et al.* (2009).

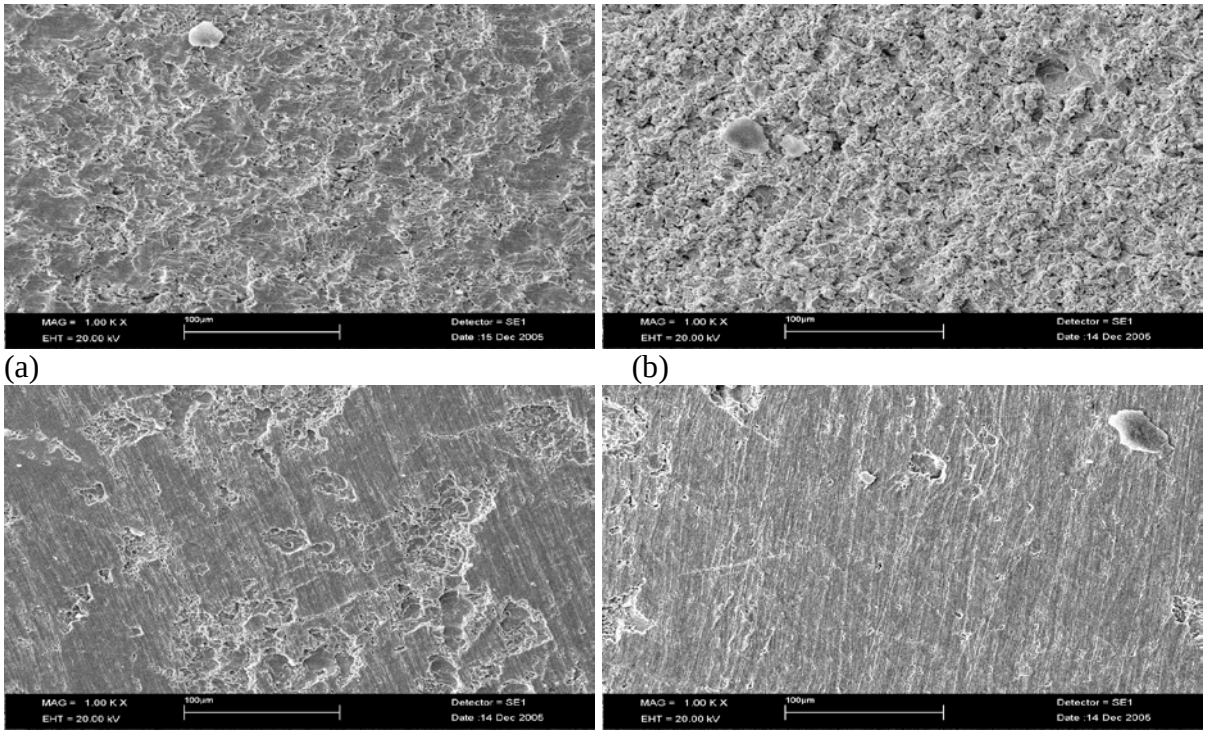

Fig. 14: Appearance of the damaged surface (a) as-received 304 stainless steel; (b) as-received 316 stainless steel; (c) Mo-304 stainless steellasersurface modified (when v = 20 mm/s); (d) Mo-304 stainless steel laser surface modified (when v = 30 mm/s); after 4 hours exposure to cavitation erosion in 3.5% NaCl solution.

Conclusion

Laser surface alloying of type 304 stainless steel with Molybdenum (Mo) had been carried out, in order to enhance its cavitation erosion resistance. This approach is economical, efficient and making engineering designs more flexible, as only the properties of the surface layer is improved while a cheaper material can be used as the bulk. Average weight (wt) % compositions of 8.86 and 11.29 of Molybdenum (Mo) were obtained within themodified layers after laser surface alloying, for when laser scanning speeds were v = 20 mm/s and v = 30 mm/s respectively. From the literature, these values are more than all % (wt) Mo composition values reported so far for any type of stainless steel, which has Mo as one of its chemical compositions. Modified surface hardness results obtained are in agreement with the existing correlation between hardness and cavitation erosion resistance. For the Mo-304 stainless steel (when v = 20 mm/s) specimen, the micro hardness of the modified layer increased from 295 HV to 359 HV (average), and for when v = 30 mm/s, it increased from 295 HV to 385 HV (average). The cavitation erosion resistance of the two modified specimens improved by a factor of 1.5 times (when v = 30 mm/s) and 1.4 times (when v = 20 mm/s) compared with that of the as-received 304 stainless steel substrate. The implication of this work is that, cost of incessant replacement of 304 stainless steel material in use due to cavitation erosion attack could be reduced, especially where they normally get in contact with high moving fluids such as in mixing processes in food and pharmaceutical industries.

References

Abouel-Kasem, A.; Emara, K.M.; Ahmed, S.M. (2009). Characterizing Cavitation Erosion Particles by Analysis of SEM Images. Tribology

International, Vol. 42 Issue 1, 130 – 136.

ASTM Standard E 384-99 (1999). Standard Test Method for Microindentation Hardness of Materials, Annual Book of ASTM Standards, ASTM, Philadelphia, PA

ASTM Standard G 32-92 (1995). Standard Method of vibratory Cavitation Erosion Test, in Annual Book of ASTM Standards, Vol. 3, No. 2, ASTM, Philadelphia.

Farnia, A., Ghaini, F.M. & Sabbaghzadeh, J. (2013). Effects of pulse duration and overlapping factor on melting ratio in preplaced pulsed Nd:YAG laser cladding, Optics and Lasers in Engineering, Vol. 51, No. 1, 69 – 76.

Fontana, M.G. (1987). Corrosion Engineering, McGraw-Hill

Frutos, A.; Arenas, M.A.; Fuentes, G.G.; Rodriguez, R.J.; Martinez, R.; Avelar-Batista, J.C. & Damborenea, J.J. (2010). Tribocorrosion behaviour of duplex surface treated AISI 304 stainless steel, Surface and Coatings Technology, Vol. 204, Nos 9-10, 1623 – 1630.

Gadag, S.P., & Srinivasan, M.N. (1995). Cavitation Erosion of Laser-Melted Ductile iron. Journal of Material Processing Technology, Vol. 51, 150-163.

Gately, N.V.H., & Dillich, S.A. (1987). Effects of titanium implantation on Cavitation erosion of Cobalt-based metal-carbide systems, Mater. Sci. Eng. Vol. 90, 333-338.

Giren, B.G. (1998). Cavitation Erosion of Steels Processed by Laser and Optical Discharge Plasma, Journal of Surface Engineering, Vol. 14, 325-330.

Guo, X., & Herman, H. (1989) in: Houek, D.L. (Ed.), Cavitation-erosion testing of thermal sprayed Tribology (T-400) coatings, in: Thermal Spray Technology: New Ideas & Processes, ASM International, Materials Park, Ohio, USA, 159.

Lovland, .P. (1993). Super Stainless Steels, Stainless steel Europe, 28 – 37.

Majumdar, J.D., Chandra, B.R., & Manna, I. (2007). Laser composite surfacing of AISI 304 stainless steel with titanium boride for improved wear resistance. Tribology International, Vol. 40, No 1, 146 – 152.

Matsumura, M., Oka, Y., Ebara, R., Kobayashi, T., Odohira, T., Wada, T. &Hatano, M. (1990). Evaluation of Cavitation –erosion resistance of ion-plated titanium nitride coating, in: Lisagor, W.B., Crooker, T.W., & Leis B.N. (Eds.), Environmentally Assisted Cracking: Science and Engineering, ASTM STP 1049, ASTM, Philadelphia, 521.

Okada, T., Iwai, I., &Awazu, K. (1988). Effects of plating on Cavitation Erosion, Wear Vol. 124, 21-31.

Richman, R.H., & McNaughton, W.P. (1990). Correlation of cavitation erosion behaviour with mechanical properties of metals, Wear Vol. 140, No 1, 63-82.

Richman, R.H., & McNaughton, W.P. (1997). A metallurgical approach to improve cavitation erosion resistance, Journal of Material Engineering Performances, Vol. 6, No. 5, 633-641.

Robinson, J.M., Anderson, S., Knutsen, R.D., & Reed, R.C. (1995). Cavitation erosion of laser melted and laser nitrided Ti-6Al-4V, Material Science Technology, Vol. 11, 611-618.

Sang, K., & Li, Y. (1995). Cavitation erosion of flame spray weld coating of nickel-based alloyed powder, Wear Vol. 189, Nos. 1-2, 20-24.

Tam, K.F, Cheng, F.T., & Man, H.C. (2002). Cavitation erosion behaviour of laser-clad Ni-Cr-Fe-WC on brass, Materials Research Bulletin Vol. 37, 1341-1351.

Tomlinson, W.J., & Bransden, A.S. (1995). Cavitation erosion of laser surface

alloyed coatings on AL-12% Si, Wear Vol. 185, Nos 1-2, 59-65.

Ushashri, K., &Manoj, M. (2015). Hard TiC Coating on AISI 304 Steel by laser surface engineering using pulsed Nd:YAG laser, Materials and Manufacturing processes, Vol. 30: 730 – 735.

Wang, B.Q., Geng, G.Q., & Levy, A.V. (1991). Effect of microstructure on the erosion-corrosion of steels, conference: Wear of Materials 1991, vol. 1, Orlando, Florida, USA, 7-11 April 1991, ASME, New York, USA, 129-136.

Wu, C.L., Zhang, S., Zhang, C.H. (2017). Phase Evolution and Cavitation Erosion-Corrosion Behavior of FeCoCrAlNiTix High Entropy Alloy Coatings on 304 Stainless Steel by Laser Surface Alloying. Journal of Alloys and Compounds, Vol. 698, 761-770.

Xu, G., Qin, M., Lei, Y. (2012). Cavitation Erosion of Cr-Ni-Mo-Cu Cladding Layer and 304 Stainless Steel. Journal of Jiangsu University Natural Science Edition, Vol. 33, No 3.

Zhang, L., Lu, J-Z., Zhang, Y-K. (2017). Effects of Laser Shock Processing on Morphologies and Mechanical Properties of ANSI 304 Stainless Steel Weldments Subjected to Cavitation Erosion. In Materials, Vol. 10, No. 3, 1996 – 1944.

Zhang, M-K., Sun, G-F., Zhang, Y-K., Liu, C-S., Ren, X-D., Feng, A-X. & Zhang W. (2014). Laser Surface Alloying of Cr-CrB_2 onto a SUS 304 Stainless Steel Substrate, Lasers in Engineering, Vol. 27, 231-245.

Zhang, S., Wu, C.L., Zhang, C.H. (2016). Laser Surface Alloying of FeCoCrAlNi High-Entropy Alloy on 304 Stainless Steel to Enhance Corrosion and Cavitation Erosion Resistances. Optics and Laser Technology, Vol. 84, 23-31.